Theoretical Study for Solvent Effect on the Potential Energy Surface for the Double Proton Transfer in Formic Acid Dimer and Formamidine Dimer

Jae-Hyun Lim,[†] **Eok Kyun Lee,**[‡] **and Yongho Kim*,**[†]

Department of Chemistry and Institute of Natural Science, Kyung Hee University, Yongin-Kun, Kyunggi-Do 449-701, Korea, and Department of Chemistry, Korea Advanced Institute of Science and Technology, Yosong-Ku, Daejon, Korea

Double proton transfers in formic acid dimer and formamidine dimer were studied as prototypes of multiple proton transfer. The potential energy surface (PES) for the double proton transfer was studied using *ab initio* quantum mechanical methods. The solvent effect on the PES was also included using the Onsager self-consistent reaction field model. In the gas phase, the transition state for the double proton transfer in the formic acid dimer complex has D_{2h} symmetry, but in water it is changed to a C_{2v} structure, when the Hartree−Fock (HF) level of theory is used. When the density functional theory is used, the transition state has D_{2h} symmetry with and without solvent. However the barrier height depends very much on the electron correlation. The double proton transfer occurs synchronously in all the cases. For the formamidine dimer complex, the transition state has C_{2v} symmetry in the gas phase, and it changes to C_s symmetry in water at the HF level of theory. The C_{2v} structure becomes an intermediate in water, which means that double proton transfer occurs asynchronously. In the density functional theory for the gas phase, the transition state has D_{2h} symmetry, and it changes to C_{2v} structure in solution. However the double proton transfer occurs synchronously in both cases. These results suggest that the correlation is very important to the PES for double proton transfer, not only in the gas phase but also in solution.

Introduction

Proton transfer is one of the simplest and the most fundamental reactions in chemistry, and it is important in oxidation−reduction reactions in many chemical and biological reactions, so it has been studied extensively.[1,2] However most of the studies of proton transfer have been done for a single proton transfer, in which one proton is transferred during the reaction. Multiproton transfers, in which more than one proton is transferred, either synchronously or asynchronously, have not been extensively studied. There are many examples of multiproton transfer such as proton relay systems in enzymes, certain proton transfers in hydrogen-bonded water complexes, and proton transfers in prototropic tautomerisms.[3] A proton relay is thought to account for the high mobility of the proton in water. Limbach *et al.* have studied the double proton transfer in prototropic tautomerisms for many formamidine systems and porphyrins using the dynamic NMR technique.[4−8] They reported rates and the kinetic isotope effects for both concerted[7,8] and stepwise[4−6] double proton transfers. However there is little theoretical work on the dynamics of multiproton transfers. To study the dynamics of such systems, one must have detailed information about potential energy surfaces near the transition state and the critical configuration. This paper presents such information for the formic acid and formamidine dimers.

Formic acid dimer (FAD) is one of most extensively studied systems both experimentally and theoretically since it forms strong hydrogen bonds, so it is fairly easy to measure its IR and Raman frequencies.[9,10] It is also one of the simplest examples of a multiproton transfer system in which the constituents are held together by two hydrogen bonds, so it can be used as a model of many chemically and biologically important multiproton transfers. Recently we have reported a

direct dynamics study for the double proton transfer in FAD.[11] Amidine compounds are important to many medical and biochemical processes.[12] They play a crucial role in the biosynthesis of imidazole and purines and the catabolism of histidine. Formamidine has been studied experimentally and theoretically as a prototype of this class of compounds. In addition to serving as a model for hydrogen transfer reactions in bases of nucleic acids, formamidine has been extensively studied theoretically since it forms homodimers and hydrogen bonds with water. Intramolecular and intermolecular hydrogen transfer have been studied theoretically for various formamidine systems.[4,5,13−16] Proton transfers in formamidine dimer can be considered a prototype of multiproton transfer. They can also provide information about hydrogen bonding, as well as the proton relay mechanism in enzymes.[3]

Because of the small mass of the proton, quantum mechanical tunneling is often very important in this reaction. The shape of the potential energy surface (PES) near the transition state and the critical configuration has influence on the tunneling probability. Most of the earlier theoretical studies have focused on the geometric change on dimerization, and the energetic stabilization due to the hydrogen bonds in the gas phase.[16] The characteristics of the PES, such as the dimerization energy and the barrier for the double proton transfer, strongly depend on the level of the theoretical calculation, the size of the basis set, and the inclusion of correlation energy.[14,16] However most proton transfers occur in solution, so the characteristics of the PES will vary with the properties of the solvent. Therefore it is necessary to understand how solvation processes influence the PES. In this study we investigated the solvent effect on the PES for the double proton transfer in formic acid dimer and in formamidine dimer, using the Hartree−Fock (HF) level of *ab initio* quantum mechanical calculation, including the self-consistent Onsager reaction field. Since electron correlation plays an important role in determining the characteristics of the

---

[†] Kyung Hee University.
[‡] Korea Advanced Institute of Science and Technology.

PES for the proton transfer reaction in the gas phase,[16,18] it is necessary to consider the correlation effect in solution too. The density functional theory has been successfully applied to the proton transfer reactions, and it agrees well with other methods including high-level electron correlation.[19] Recently Ruiz-López *et al.* have studied solvent effects on the proton transfer using density function theory including the self-consistent Onsager reaction field, and they showed that the solute's correlation energy could be greatly modified in the solvation process.[20] We have performed density functional theory calculations to investigate the change in the PES, compared with the HF calculation without the correlation effect, in the gas phase and in solution.

Calculations

All electronic structure calculations were done using the GAUSSIAN 94 quantum mechanical packages.[21] Geometries for formic acid (FA), formamidine (FD), stable formic acid dimer (FAD), formamidine dimer (FDD), and the transition states for the double proton transfer in formic acid dimer and formamidine dimer were optimized at the Hartree−Fock (HF) level of theory using the 6-31G(d,p) basis set. Density functional theory calculations were also performed. Becke's three-parameter[22] gradient-corrected exchange with the Lee−Yang−Parr[23] gradient-corrected correlation (B3LYP) using the 6-31G(d,p) basis set was employed.

The self-consistent Onsager reaction field model[24] was used to optimize structures and to calculate energies for various dielectric constants. Frequencies were calculated for all bound and transition state structures. The imaginary frequency at the transition state has been monitored with the variation of the dielectric constant. In the Onsager reaction field theory,[24] the solute in a spherical cavity is surrounded by a polarizable medium with a dielectric constant ϵ. A dipole in the solute induces a dipole in the medium, and the electric field applied to the solute by the solvent dipole will interact with the solute dipole to produce net stabilization. In the quantum mechanical theory, the solvent effect is taken as a perturbation term, H_1, in the Hamiltonian of the isolated solute, H_0:[25,26]

$$H = H_0 + H_1 \tag{1}$$

The perturbation term (H_1) represents the coupling between the reaction field vector, $\vec{R}$ and the electric dipole moment operator, $\vec{\mu}$:

$$H_1 = -\vec{\mu} \cdot \vec{R} \tag{2}$$

The reaction field, $\vec{R}$, is proportional to the electric dipole moment, $\vec{\mu}$:

$$\vec{R} = -g \cdot \vec{\mu} \tag{3}$$

The proportionality constant, g, is the Onsager factor, which determines the strength of the reaction field. It depends on the dielectric constant of the medium, ϵ, and on the radius of the cavity, a_0:

$$g = \frac{2(\epsilon - 1)}{(2\epsilon + 1)a_0^3} \tag{4}$$

The effect of the reaction field by the solvent perturbation is incorporated as an additional term in the Fock equation:

$$F = F^0 - g\vec{\mu} \cdot \langle \vec{\mu} \rangle \tag{5}$$

The energy is given by

$$E = \langle \Psi | H_0 | \Psi \rangle - 0.5\vec{\mu} \cdot \vec{R} \tag{6}$$

where Ψ is the full wave function of the molecule. These self-consistent reaction field (SCRF) equations are solved iteratively.

The cavity radius is the only adjustable parameters in a solvent effect calculation, and the choice of the radius has been discussed extensively.[25−28] The simplest method to obtain the radius is to calculate it from the solute molar volume (V_m):

$$a_0^3 = 3V_m/4\pi N_A \tag{8}$$

in which V_m is given by experiment and N_A is Avogadro's number. When the experimental molar volume is not available, the molecular greatest dimension could be used to estimate the radius.[26] In this approach, the diameter of the molecule is calculated from the largest internuclear distance by adding the van der Waals radii of the two end atoms involved. Then, the radius obtained by this approach is increased by 0.5 Å to account for the van der Waals radii of the surrounding solvent molecules. In this study, the radius was calculated from the molecular volume of the optimized structure in the gas phase, on the assumption that the structure is spherical, and increased by 0.5 Å to consider the surrounding solvent molecules. This method is implemented in the GAUSSIAN 94 *ab initio* quantum mechanical package[21] that was used for all electronic geometry calculations.

The dimerization energies for the hydrogen-bonded complexes were calculated from the difference in energies between the dimer and two monomers. The basis set superposition error (BSSE) may be important in the calculation of the dimerization energies.[29] The BSSE was corrected by the Boys and Bernardi counterpoise correction scheme,[15,30]

$$\text{BSSE} = 2[E_m(M) - E_d(M')] + E_{reorg} \tag{9}$$

$$E_{reorg} = 2[E_m(M') - E_m(M)] \tag{10}$$

where $E_m(M)$ and $E_d(M')$ are the energies of the monomer in its own basis set and in the basis set of the dimer, respectively, and M and M′ denote the optimized geometry of monomer and the geometry of the monomer in the optimized dimer, respectively. The reorganization energy (E_{reorg}), i.e., the energy associated with the transition from the optimized geometry of monomer to the geometry that the monomer has in the dimer, should also be included in the correction of the BSSE. The corrected dimerization energy is determined as follows:

$$E_d(\text{corr}) = E(D) - 2E_m(M) + \text{BSSE} \tag{11}$$

$$= E(D) - 2E_d(M') + E_{reorg}$$

where $E(D)$ is the energy of dimer.

Results and Discussion

Formic Acid Dimer. The geometries for FA, FAD, and the transition state (FADTS) for the double proton transfer were optimized at the HF level of theory and at the B3LYP density functional level. They are shown in Figure 1. FAD has C_{2h} symmetry in the gas phase with two hydrogen bonds. The O−H bond length in FAD is 0.014 Å longer than the O−H bond length in FA due to the hydrogen bond at the HF level of theory. The same bond length at the B3LYP level of theory is 0.124 Å longer than that in FA. The bond distance for the hydrogen bond in the density functional theory is 1.643 Å, which is about 0.2 Å shorter than that at the HF level of theory. The experimental distance for the hydrogen bond is 1.663 Å,[17] which agrees very well with the B3LYP results. The density functional theory predicts slightly larger bond lengths for all bonds except the hydrogen bond in FAD. A transition state structure with
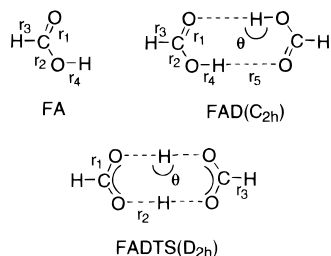
Figure 1. Geometries for FA, FAD, and FADTS. Numbers in parentheses are from the geometries obtained at the density functional theory (B3LYP). The unparenthesized numbers are from the HF calculation. FA: $r_1 = 1.182(1.230)$, $r_2 = 1.322(1.346)$, $r_3 = 1.085(1.100)$, $r_4 = 0.949(0.974)$. FAD: $r_1 = 1.196(1.227)$, $r_2 = 1.298(1.310)$, $r_3 = 1.084(1.007)$, $r_4 = 0.963(1.098)$; $r_5 = 1.831(1.643)$, $\theta = 173.5(178.9)$. FDDTS: $r_1 = 1.242(1.264)$, $r_2 = 1.118(1.210)$, $r_3 = 1.084(1.098)$, $\theta = 179.1(178.6)$. Experimental bond lengths and angles are as follows.[17] FA: $r_1 = 1.202$, $r_2 = 1.343$, $r_3 = 1.097$, $r_4 = 0.972$. FAD: $r_1 = 1.217$, $r_2 = 1.320$, $r_3 = 1.079$, $r_4 = 1.033$, $r_5 = 1.663$, $\theta = 180°$ (assumed). Bond lengths are in angstroms, angles in degrees.

TABLE 1: Dimerization Energies, Barrier Heights for the Double Proton Transfer in FAD, and Imaginary Frequencies of FADTS(D_{2h}) at Various Levels of Theory in the Gas Phase[a]

	$E_d{}^b$	$E^{\ddagger c}$	$\nu^{\ddagger d}$	ref
HF/STO-3G	−15.2	5.2	1078i	31c
HF/6-31G	−19.1	15.6	1743i	31c
HF/6-31+G	−13.6	17.1	1760i	31c
MP2/6-31G(d,p)	−18.4	8.0	1341i	31c
HF/DZ	−19.3(−16.8)	14.2	1663i	31a
HF/DZ+P	−14.3(−12.3)	15.6	1695i	31a
HF/6-31+G(d,p)	−13.6	17.1		11
HF/6-311G(d,p)	−14.4	18.0		11
HF/6-311+G(d,p)	−12.9	18.4		11
B3LYP/cc-pVDZ	−20.8	5.2		11
B3LYP/AUG-cc-pVDZ	−15.7	6.3		11
G2*	−16.2(−14.2)	8.94(5.20)		11
MCPF	−16.2(−13.9)	12.0		31b
HF/6-31G(d,p)	−15.3(−11.1[e])	16.6(11.2)	1756i	this study
B3LYP/6-31G(d,p)	−19.6(−13.7[e])	5.4(1.51)	1195i	this study
expt	−14.4			32

[a] Numbers in parentheses are with zero-point energy. [b] Relative energies of FAD with respect to the energies of two FA in kcal mol⁻¹. [c] Relative energies of FADTS with respect to the energies of FAD in kcal mol⁻¹. [d] Reaction coordinate frequency in cm⁻¹. [e] The BSSEs are corrected in addition to zero-point energy.

D_{2h} symmetry is obtained at both the HF and the B3LYP level of theories in the gas phase. This result suggests that the double proton transfer proceeds through a concerted mechanism in the gas phase. The geometries from the B3LYP method for FA, FAD, and FADTS agree better than those from the HF calculation with the experimental[17] and high-level *ab initio* results including electron correlation.[11]

Dimerization energies, barrier heights, and imaginary frequencies are listed in Table 1 for the gas phase. Dimerization energies and barrier heights are changed very much with the level of theory and the size of the basis sets.[31] Electron correlation is very important in determining dimerization energies and barrier heights. Adding diffuse functions to the basis set does not improve the results at the HF level of theory. The calculated dimerization energies, without any zero-point energy correction, are −15.3 and −19.6 kcal mol⁻¹, from the HF and the B3LYP methods, respectively. They are −13.3 and −17.8 kcal mol⁻¹, from the HF and the B3LYP methods, respectively, with zero-point energy correction. The experimental enthalpy of dimerization for FAD is about −14.4 kcal mol⁻¹.[32] Scheiner has reported that the basis set superposition errors (BSSEs) may be important in the determination of the dimerization energy for hydrogen-bonded complexes.[29] There

TABLE 2: Dimerization Energies for the Double Proton Transfer in FAD, and Frequencies of FADTS(D_{2h}) at the HF and B3LYP Level of Theories with the Onsager Reaction Field Model at Various Dielectric Constants[a]

ϵ	$E_d{}^b$	$\nu^{\ddagger}(B_{3g})^c$	$\nu(B_{1u})^d$
gas	−15.3(−19.6)	1756i (1195i)	768 (1362)
2	−14.6(−19.2)	1756i (1195i)	565 (1282)
5	−13.7(−18.8)	1756i (1195i)	120 (1170)
10	−13.7(−18.6)	1756i (1195i)	348i (1117)
20	−13.7(−18.5)	1756i (1195i)	444i (1075)
40	−13.7(−18.4)	1756i (1195i)	487i (1069)
78.4	−13.7(−18.4)	1756i (1195i)	509i (1060)

[a] Numbers in parentheses are from the B3LYP method. The barrier heights for the double proton transfer in FAD at the HF and B3LYP levels of theory are 16.6 and 5.4 kcal mol⁻¹, respectively, and these values are not changed by solvent effect. The cavity radii for FA, FAD, and FADTS(D_{2h}) are 3.05, 3.69, and 3.49 Å, respectively, for the HF method, and 3.04, 3.58, and 3.47 Å, respectively, for the B3LYP method. [b] Relative energies of FAD with respect to the energies of two FA in kcal mol⁻¹. The BSSEs are not corrected. [c] Reaction coordinate frequency in cm⁻¹. [d] The normal mode frequency most sensitive to the solvent polarity. Other frequencies are almost insensitive to the solvent polarity.

may be the BSSEs involved in the dimerization energies in Table 1, which make the dimerization energies less negative. The counterpoise procedure was performed to correct the BSSE for the dimerization energies in the gas phase. The BSSEs from the HF and the B3LYP methods are 2.19 and 4.08 kcal mol⁻¹, respectively. From eq 11, the corrected dimerization energies from the HF and the B3LYP methods are −11.1 and −13.7 kcal mol⁻¹, respectively, with zero-point energy correction. The corrected dimerization energy from the B3LYP method agrees very well with the experimental value. The barrier heights were calculated from the difference in energies between FADTS with D_{2h} symmetry and FAD. The calculated barrier heights from the HF and the B3LYP methods are 16.6 and 5.42 kcal mol⁻¹, respectively. The value from the HF method is larger, but that from the B3LYP method is smaller than the barrier height from the G2* level of theory,[11] which is 8.94 kcal mol⁻¹. The B3LYP method slightly underestimates the barrier height, but the value from the B3LYP method agrees with the G2* values better.

The geometries of FA, FAD, and FADTS with D_{2h} symmetry have been optimized in solution at various dielectric constants. Dimerization energies and frequencies are listed in Table 2 for solutions with various dielectric constants. The calculated dimerization energy becomes less negative as the dielectric constant increases. The global dipole moment of FAD is zero because it has C_{2h} symmetry, and this gives zero reaction field in eq 3. Therefore there is no stabilization in energy for FAD by the Onsager self-consistent reaction field method (eqs 1−6). The change in the dimerization energy is due to the stabilization of the monomer in solution, which makes the dimerization energy less negative. However the change is not large: only about 1.6 kcal mol⁻¹ at the HF level of theory, and 2.3 kcal mol⁻¹ at the B3LYP level of theory. These results suggest that the strong hydrogen bonds in FAD are not weakened very much even in a very polar solvent. However this does not take more specific interactions into account. For example, formic acid does not dimerize in dilute aqueous solution. Therefore these results are meaningful in solutions such that solvent provides a polar dielectric medium to solute without specific interactions.

The calculated imaginary reaction coordinate frequency with B_{3g} symmetry is insensitive to the dielectric constant, but the frequency with B_{1u} symmetry is very sensitive; in particular the B_{1u} frequency from the HF method becomes imaginary between dielectric constants of 5 and 10. These results indicate that the FADTS with D_{2h} symmetry is not a real transition state,
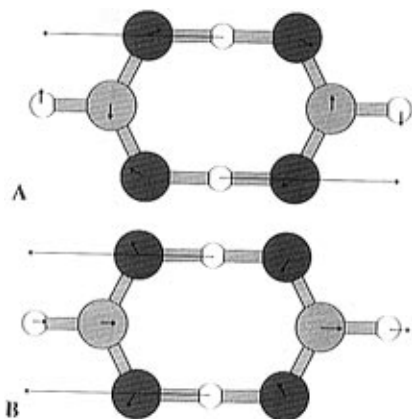
Figure 2. Normal mode eigenvectors for FADTS(D_{2h}) optimized at the HF level of theory using the Onsager reaction field model for water. (A) Normal mode eigenvector for the reaction coordinate frequency (B_{3g}). (B) Normal mode eigenvector for the frequency with B_{1u} symmetry, which is sensitive to the strength of the reaction field.
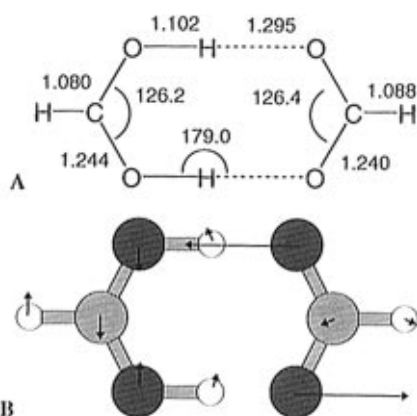

Figure 3. C_{2v} transition state structure optimized at the HF level of theory using the Onsager self-consistent reaction field model for water and the eigenvectors for the reaction coordinate frequency.

but just a stationary point on the PES, in highly polar solvents at the HF level of theory. The eigenvectors for the B_{3g} and B_{1u} frequencies are shown in Figure 2. The B_{3g} normal mode of the reaction coordinate does not change the dipole moment of the FADTS. However the B_{1u} normal mode vibration changes the dipole moment of FADTS greatly. The large change in the dipole moment due to this vibrational motion influences the reaction field; therefore the B_{1u} frequency is sensitive to the strength of reaction field, which is related to the dielectric constant. The frequency becomes imaginary because the potential curve for the B_{1u} vibrational motion is inverted in a polar solvent. This is not surprising since the B_{1u} mode induces a large dipole moment at the turning point of vibration, where the total energy can be reduced by solvation. The real transition state structure in a medium with the water dielectric constant was calculated at the HF level of theory. It has C_{2v} symmetry, as shown in Figure 3. The reaction coordinate frequency is 1276i cm^{-1} and this is the only imaginary frequency. The eigenvector for the reaction coordinate is also shown in Figure 3. The barrier heights, dipole moments, and the reaction coordinate frequencies for the C_{2v} FADTS at various dielectric constants are listed in Table 3. The positions of the two protons in flight are shifted continuously toward one formate residue as the dielectric constant is increased. The dipole moment is increased at the same time. The barrier height in the high permittivity fluid is reduced by only 0.1 kcal mol^{-1} compared with the barrier in the gas phase, which suggests that the solvation process does not have a big influence on the barrier height. The energies of the C_{2v} structure

TABLE 3: Barrier Heights and Reaction Coordinate Frequencies of FADTS(C_{2v}) at the HF Level of Theory with the Onsager Reaction Field Model at Various Dielectric Constants[a]

ϵ	$E^{\ddagger b}$	$\nu^{\ddagger}(B_2)^c$	$\nu(A_1)^d$	Δr^e	μ^f
gas[g]	16.638	1756i	768	0.0	0.00
2	16.641	1748i	530	0.020	0.21
5	16.639	1747i	189	0.020	0.23
10	16.616	1510i	981	0.140	1.60
20	16.582	1280i	1204	0.192	2.21
40	16.552	1279i	1193	0.192	2.22
78.4	16.537	1276i	1189	0.193	2.24

[a] The structures of FADTS(C_{2v}) were optimized at each dielectric constant with the cavity radius of 3.49 Å. [b] Relative energies of FADTS(C_{2v}) with respect to the energies of FAD in kcal mol^{-1}. [c] Reaction coordinate frequency in cm^{-1}. [d] Frequencies that are similar to the normal mode vibration as the B_{1u} mode in FADTS with D_{2h} symmetry. [e] The difference between two O–H bond lengths ($r_1 - r_2$ in fig. 4) in FADTS(C_{2v}) in angstroms. [f] Dipole moments in debyes. [g] In the gas phase, FADTS has D_{2h} symmetry.
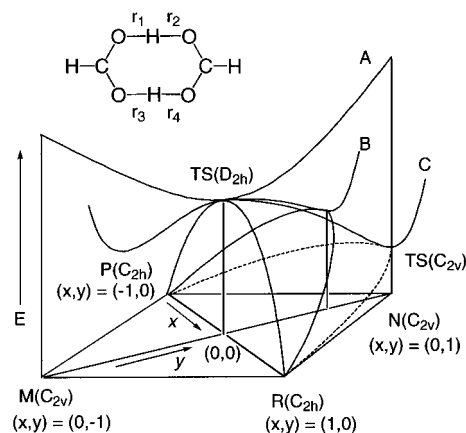

Figure 4. Schematic three-dimensional diagram for the solvent effect on the PES for the double proton transfer in FAD at the HF level of theory. R and P represent the structures for the FAD complex, and M and N represent the FADTS(C_{2v}) structures in water. The "x" represents the reaction coordinate connecting R and P, and the "y" represents the coordinate for the normal mode vibration with B_{1u} symmetry perpendicular to the reaction coordinate connecting M and N. The variables "x" and "y" are defined in the text. The lines "A", "B", and "C" are schematic potential curves for the normal mode vibration with B_{1u} symmetry in the gas phase, in an intermediately polar solvent, and in water, respectively. The left half of the curve "C" is not shown. The minimum energy reaction coordinate in water is along the line connecting R, TS$_2$, and P.

at $\epsilon = 2$ and 5 are slightly larger than those in the gas phase. These results mean that the reaction path via a C_{2v} FADTS structure is not a minimum energy path at $\epsilon = 2$ and 5, so the real transition state in these cases is the structure with D_{2h} symmetry. This is consistent with the fact that the B_{1u} frequencies in the D_{2h} structure do not become imaginary until $\epsilon = 10$, as shown in Table 2.

The solvent effect on the PES for the double proton transfer in FAD at the HF level of theory is schematically shown in Figure 4. The reaction coordinate variable, x, and the variable that represents a normal mode with B_{1u} symmetry, y, can be defined approximately as eqs. 12 and 13,

$$x = \frac{(r_1 + r_4) - (r_2 + r_3)}{(r_1^d + r_4^d) - (r_2^d + r_3^d)} \tag{12}$$

$$y = \frac{(r_1 + r_3) - (r_2 + r_4)}{(r_1^w + r_3^w) - (r_2^w + r_4^w)} \tag{13}$$

where r's are bond distances as defined in Figure 4 and r^d's

Double Proton Transfer in Formic Acid Dimer

J. Phys. Chem. A, Vol. 101, No. 12, 1997 **2237**

and r^w's are the corresponding distances in the FAD complex and the C_{2v} structure of FADTS, respectively, in water, which are given in Figures 1 and 3A. The ideal potential curve, A, in Figure 4, for the normal mode vibration (B_{1u}) perpendicular to the reaction coordinate becomes inverted in a polar solvent, as shown in the potential curves, B and C. This changes the minimum energy reaction coordinate from the path via TS(D_{2h}) in the gas phase to the path via TS$_2$(C_{2v}) in water. The C_{2v} structure in water is not an intermediate. It is the transition state with an imaginary frequency, which means that the double proton transfer occurs synchronously.

In the density functional theory the B_{1u} frequency is larger than that from the HF level of theory, which means that the potential curve for the B_{1u} vibrational motion is steeper. It is not inverted even in water, even though the frequency becomes smaller with increasing the dielectric constants. This means that the potential curve for the B_{1u} mode from the B3LYP method is fairly stiff. The D_{2h} structure for FADTS has only one imaginary frequency in all cases, as shown in Table 2. The fact that the imaginary frequency is not varied with solvation indicates that the minimum energy reaction path for the double proton transfer is not changed with the permittivity of the medium. This result can be understood since the double proton transfer, as shown in Figure 2A, does not change the dipole moment of reaction and the strength of the reaction field. The reaction occurs through a D_{2h} transition state both in the gas phase and in solution. The solvent effect on the PES from the density functional theory (B3LYP) is quite different from that predicted by the HF level of theory. This difference originates probably from the fact that the HF level of MO theory does not include electron correlation. Therefore electron correlation is very important in determining the reaction coordinate for the double proton transfer in solution.

Formamidine Dimer. The geometries for FD, FDD, and the transition state for the double proton transfer (FDDTS) are optimized at the HF level of theory, and the geometric parameters are shown in Figure 5. The optimized structure of FDD has C_i symmetry. Truhlar and co-workers have reported a slightly different optimized structure for FDD (a C_2 structure),[16a] but the difference between the energies of these structures is less than 0.1 kcal mol^{-1}, and the geometries of two conformers are very similar. It is not necessary to consider all structures for a solvent effect study, so we used only the C_i structure for the solvent effect calculation.

The D_{2h} structure of FDDTS from the HF level of theory has two imaginary frequencies both in the gas phase and in solution, which means that this structure is not a real transition state for the double proton transfer. Ahlberg and co-workers have reported that the C_{2v} structure is an intermediate at the HF level of theory using the 6-31G(d) basis sets.[16b] However, the C_{2v} structure in this study is a transition state with one imaginary frequency in the gas phase. The dimerization energies, barrier heights, transition state symmetries, and imaginary frequencies, at the various level of theories in gas phase, are listed in Table 4. Not only the dimerization energies and the barrier heights but also the symmetry of the transition state are changed very much with the level of theories and the size of the basis sets. The BSSEs in the dimerization energies were corrected from the HF and B3LYP methods using eq 9, and they are 1.72 and 3.54 kcal mol^{-1}, respectively. The corrected dimerization energies including the BSSEs and zero-point energies from the HF and B3LYP methods are −8.14 and −12.1 kcal mol^{-1}, respectively. The dimerization energy and the barrier height from the B3LYP method agree very well with those from the high-level *ab initio* calculations including electron correlation. Electron correlation changes the transition state
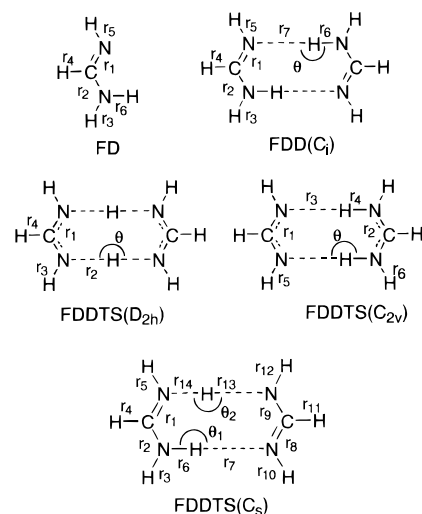

Figure 5. Geometries for FD, FDD, and FDDTS(D_{2h}) optimized at the HF and B3LYP level of theory in the gas phase. Numbers in parentheses are from the B3LYP results. Bond lengths are in angstroms and angles in degrees. FD: $r_1 = 1.255(1.277)$, $r_2 = 1.368(1.376)$, $r_3 = 0.993(1.009)$, $r_4 = 1.085(1.099)$, $r_5 = 1.001(1.020)$, $r_6 = 0.995(1.012)$. FDD: $r_1 = 1.266(1.292)$, $r_2 = 1.345(1.347)$, $r_3 = 0.991(1.005)$, $r_4 = 1.086(1.098)$, $r_5 = 1.001(1.017)$, $r_6 = 1.006(1.035)$, $r_7 = 2.103(1.894)$, $\theta = 175.6(174.5)$. FDDTS(D_{2h}): $r_1 = 1.302(1.318)$, $r_2 = 1.277(1.288)$, $r_3 = 0.996(1.011)$, $r_4 = 1.086(1.098)$, $\theta = 174.0(174.2)$. The geometries for FDDTS(C_{2v}) are optimized at the HF level of theory in the gas phase and at the B3LYP level of theory in water. The geometry for FDDTS(C_s) is optimized at the HF level of theory in water. FDDTS-(C_{2v}): $r_1 = 1.305(1.321)$, $r_2 = 1.297(1.315)$, $r_3 = 1.572(1.520)$, $r_4 = 1.090(1.129)$, $r_5 = 0.999(1.014)$, $r_6 = 0.993(1.010)$, $\theta = 174.1(174.0)$. FDDTS(C_S): $r_1 = 1.288$, $r_2 = 1.309$, $r_3 = 0.992$, $r_4 = 1.079$, $r_5 = 0.995$, $r_6 = 1.029$, $r_7 = 1.831$, $r_8 = 1.295$, $r_9 = 1.313$, $r_{10} = 1.000$, $r_{11} = 1.096$, $r_{12} = 0.998$, $r_{13} = 1.441$, $r_{14} = 1.152$, $\theta_1 = 170.3$, $\theta_2 = 177.1$.

symmetries as well as the dimerization energies and the barrier heights. These results suggest that electron correlation should be considered in the calculation of the PES for the double proton transfer in FDD, not only in the gas phase but also in solution.

The dimerization energies, the barrier heights, and the reaction coordinate frequencies in media of various dielectric constants at the HF level of theory are listed in Table 5. The dimerization energies are reduced about 3.3 kcal mol^{-1} by solvation, because the energy of FD is lowered by solvation, but that of FDD is not, because of its zero dipole moment. The C_{2v} structure of FDDTS becomes an intermediate in solution, because the imaginary frequency disappears in a solvent with $\epsilon = 2.0$, as shown in Table 5. This result means that the double proton transfer in solution occurs via a stepwise mechanism, with an intermediate of C_{2v} symmetry, at the HF level of theory. Since the positions of the two protons are already shifted toward the nitrogens of one monomer unit in the gas phase, the dipole moment of the transition state is fairly large, about 4.6 D. As the dielectric constants are increased, the bridging protons are shifted further; therefore the dipole moment of the C_{2v} inter-mediate that is formed by a single proton transfer becomes even larger, as listed in Table 5. This stabilizes the FDDTS(C_{2v}) and reduces the barrier height about 4.1 kcal mol^{-1}. Since the C_{2v} structure is an intermediate and the proton transfer occurs stepwise, there must exist two transition states for each step of the reaction. The transition state for the single proton transfer at the HF level of theory was calculated in water, and it has C_s symmetry, as shown in Figure 5. The other transition state is just the mirror image of this structure, and the barrier height is 20.391 kcal mol^{-1} in water. The C_{2v} intermediate in water is only 0.672 kcal mol^{-1} lower in energy than the C_s transition state. The concerted double proton transfer in the gas phase has switched to stepwise in water with about 3.4 kcal mol^{-1} of

TABLE 4: Dimerization Energies, Barrier Heights, Transition State Symmetry, and Imaginary Frequencies for the Double Proton Transfer in FDD in the Gas Phase[a]

	$E_d{}^b$	$E^{\ddagger c}$	TS symm	$\nu^{\ddagger d}$	ref
HF/STO-3G	−11.7	9.0	C_{2v}	1311i	16b
HF/3-21G	−19.9	16.0	C_{2v}	1494i	16b
HF/6-31G	−14.3	19.4	C_{2v}	432i	16b
HF/6-31+G	−12.8	19.4	C_{2v}	146i	16b
HF/6-31G(d)	−11.2(−9.6)	25.4(23.0)	C_s	328i	16a
MP2/6-31G(d,p)//HF/6-31G(d,p)	−15.4(−13.9)	13.8(8.1)	D_{2h}		16a
SAC2/6-31G(d,p)//HF/6-31G(d,p)		11.0(5.3)	D_{2h}		16a
HF/6-31G(d,p)	−11.4(−8.14[e])	23.8(21.5)	C_{2v}	231i	this study
B3LYP/6-31G(d,p)	−16.6(−12.1[e])	11.7(6.78)	D_{2h}	1462i	this study

[a] Numbers in parentheses are with zero-point energy. [b] Relative energies of FDD with respect to the energies of two FD in kcal mol^{-1}. [c] Relative energies of FDDTS with respect to the energies of FDD in kcal mol^{-1}. [d] Reaction coordinate frequency in cm^{-1}. [e] The BSSEs are corrected in addition to zero-point energy.

TABLE 5: Dimerization Energies, Barrier Heights for the Double Proton Transfer in FDD, and Frequencies of FDDTS(C_{2v}) at the HF Level of Theory with the Onsager Reaction Field Model at Various Dielectric Constants[a]

ϵ	$E_d{}^b$	$E^{\ddagger c}$	$\nu(B_2)^d$	Δr^e	μ^f
gas	−11.444	23.825	231i	0.482	4.65
2	−10.215	22.564	105	0.550	5.54
5	−9.090	21.147	186	0.612	6.39
10	−8.611	20.458	196	0.640	6.78
20	−8.346	20.053	200	0.654	6.99
40	−8.205	19.832	203	0.665	7.13
78.4	−8.134	19.719	203	0.668	7.18

[a] The cavity radii for FD, FDD, and FDDTS(C_{2v}) are 3.40, 3.99, and 3.89 Å, respectively. [b] Relative energies of FDD with respect to the energies of two FD in kcal mol^{-1}. The BSSEs are not corrected. [c] Relative energies of FDDTS(C_{2v}) with respect to the energies of FDD in kcal mol^{-1}. [d] Reaction coordinate frequency in cm^{-1}. This becomes nonimaginary in solution. [e] The difference between two N−H bond lengths ($r_3 − r_4$ in FDDTS(C_{2v}) of Figure 5) in angstroms. [f] Dipole moments in debyes.

TABLE 6: Dimerization Energies, Barrier Heights for the Double Proton Transfer in FDD, and Frequencies of FDDTS at the B3LYP Level of Theory with the Onsager Reaction Field Model at Various Dielectric Constants[a]

		D_{2h}		C_{2v}	
ϵ	$E_d{}^b$	$\nu(B_{3g})^c$	$\nu(B_{1u})^d$	$E^{\ddagger e}$	$\nu(B_2)^f$
gas	−16.637	1462i	446	g	g
2	−15.605	1462i	107i	11.683	1366i
5	−14.652	1462i	464i	11.426	743i
10	−14.242	1462i	553i	11.190	478i
20	−14.014	1462i	597i	11.022	349i
40	−13.893	1462i	620i	10.923	287i
78.4	−13.832	1462i	631i	10.869	285i

[a] The cavity radii for FD, FDD, FDDTS(D_{2h}), and FDDTS(C_{2v}) are 3.40, 3.88, 3.84(D_{2h}), and 3.67(C_{2v}) Å, respectively. The barrier height, which is the relative energy of FDDTS(D_{2h}) with respect to the energy of FDD, is 11.69 kcal mol^{-1}, and this is not changed with dielectric constants. [b] Relative energies of FDD with respect to the energies of two FD in kcal mol^{-1}. The BSSEs are not corrected. [c] Reaction coordinate frequency of FDDTS(D_{2h}) in cm^{-1}. [d] The normal mode frequency of FDDTS(D_{2h}) most sensitive to the solvent polarity. Other frequencies are almost insensitive to the solvent polarity. [e] Relative energies of FDDTS(C_{2v}) with respect to the energies of FDD in kcal mol^{-1}. [f] Reaction coordinate frequency of FDDTS(C_{2v}) in cm^{-1}. [g] In the gas phase, the transition state has D_{2h} symmetry.

advantage in energy by solvation. The bond distances, r_{14} and r_{13} in FDDTS(C_s) of Figure 5, are 1.152 and 1.441 Å, respectively, which suggest that the C_s structure is more similar to the C_{2v} intermediate than to FDD(C_i).

The geometries for FD, FDD, and FDDTS, optimized at the B3LYP level of theory, are also shown in Figure 5. The hydrogen bond length in FDD, r_7, is about 0.21 Å shorter than that from the HF method. This indicates that the hydrogen bonds from the B3LYP method are stronger. This result is consistent with the results for the FAD, in which the dimerization energy obtained from the B3LYP method is more negative than that from the HF method, as shown in Table 2. The geometry for the FDDTS in the gas phase has D_{2h} symmetry, with an imaginary frequency as shown in Figure 5. The barrier height and the dimerization energy in the gas phase are 11.69 and −16.64 kcal mol^{-1}, respectively, which agree very well with previous high-level *ab initio* calculation including the electron correlation.[16a] There are two imaginary frequencies for the FDDTS(D_{2h}) in solution for all dielectric constants of 2 and above, which shows that FDDTS(D_{2h}) is not a real transition state. The transition state given by the B3LYP calculation for the double proton transfer in solution has C_{2v} symmetry, and this structure is also shown in Figure 5. The barrier heights and imaginary frequencies at various dielectric constants are shown in Table 6. The dimerization energy is less negative by about 2.8 kcal mol^{-1}. This occurs because only the energy of FD is lowered by solvation, as mentioned before. The imaginary frequency of the FDDTS(C_{2v}) in solution becomes much smaller with increasing dielectric constant, but it still remains imaginary in water. This means that FDDTS(C_{2v}) is not an intermediate even in water, and it is a real transition state for the concerted double proton transfer. The barrier height is reduced by about 0.82 kcal mol^{-1} in a medium with the water dielectric constant

compared with that in the gas phase, which suggests that dielectric solvation does not have much influence on the barrier height in the density functional theory. Limbach *et al.* have measured Arrhenius activation energy for the double proton transfer in N,N′-bis(p-fluorophenyl)formamidine dimer in THF, which is 4.52 kcal mol^{-1}.[7] The calculated thermal energies for FDD and FDDTS(C_{2v}) at the B3LYP level of theory in a medium of $\epsilon = 10$, including vibrational, rotational, and translational energies, are 79.77 and 73.54 kcal mol^{-1}, respectively, at 298 K. The enthalpy of activation, estimated from the thermal energies and the barrier height, is 4.95 kcal mol^{-1}, which agrees very well with the experimental value.

A schematic diagram of the potential energy surface for the double proton transfer in formamidine dimer is shown in Figure 6. Imaginable reaction paths for the double proton transfer are from R(C_i) to P(C_i) via either TS(D_{2h}), TS(C_{2v}), or I(C_{2v}). At the HF level of theory in the gas phase, the double proton transfer occurs synchronously via TS(C_{2v}); however in solution, the proton transfer occurs asynchronously via I(C_{2v}). There are two transition states, both with C_s symmetry, at the top of the dashed lines in Figure 6. These two transition states have a mirror image relation. At the density functional level of theory, in the gas phase, the double proton transfer occurs synchronously via TS(D_{2h}). In solution, it occurs synchronously too, but via TS(C_{2v}). The C_{2v} structure is not an intermediate in this case. The two theories (HF and B3LYP) produce quite different results both in the gas phase and in solution. Most importantly, the HF method predicts a stepwise reaction path for the double
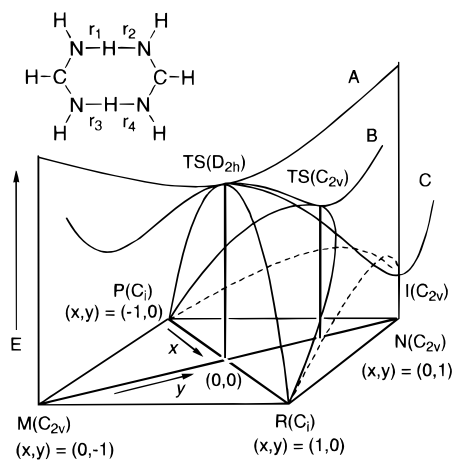
Double Proton Transfer in Formic Acid Dimer

J. Phys. Chem. A, Vol. 101, No. 12, 1997 **2239**

Figure 6. Schematic three-dimensional diagram for the solvent effect on the PES for the double proton transfer in FDD. R and P represent the structures for the FDD complex, and M and N represent the C_{2v} structures in water. The "x" represents the reaction coordinate connecting R and P, and the "y" represents the coordinate for the normal mode vibration with B_{1u} symmetry perpendicular to the reaction coordinate connecting M and N. The variables "x" and "y" are defined in the text. The lines "A", "B", and "C" are schematic potential curves for the normal mode vibration with B_{1u} symmetry in the gas phase-(B3LYP), in a polar solvent(B3LYP), and in water(HF), respectively. The left half of the curve "C" is not shown. The minimum energy reaction coordinate from the HF method in water is along the dashed line connecting R, I, and P.

proton transfer in solution, but the B3LYP method predicts a concerted path. These differences are probably due to the fact that the HF level of MO theory does not include electron correlation; therefore these results suggest that the electron correlation is very important in calculating the PES for the double proton transfer, not only in the gas phase but also in solution. Since very many important proton transfer reactions occur in solution, it is crucial to understand how the PES is modified by a polar solvent. This study shows that correlation should be included in estimating the PES for double proton transfer in solution.

Concluding Remarks

The PESs for the double proton transfer in formic acid dimer and in formamidine dimer have been studied at the HF and the density functional levels of theory, with and without a medium effect. The double proton transfer in formic acid dimer occurs synchronously with a D_{2h} transition state both in the gas phase and in solution at the B3LYP level of theory. At the HF level of theory, however, the transition state is changed from a D_{2h} structure in the gas phase to a C_{2v} structure in solution, even though the double proton transfer occurs synchronously.

The double proton transfer in formamidine dimer occurs via a concerted mechanism through a D_{2h} transition state in the gas phase, and a C_{2v} transition state in solution in the density functional theory. At the HF level of theory, however, the mechanism of the double proton transfer changes with solvent. In the gas phase, the double proton transfer occurs via a concerted mechanism through a C_{2v} transition state, but in solution it occurs via a stepwise mechanism through a C_s transition state and a C_{2v} intermediate. The solvent effect on the PES for double proton transfer is very important. Correlation turns out to be crucial to the PES for the double proton transfer in the gas phase and also in solution. Density functional

theory with the SCRF method can be used to study the medium effect successfully.

References and Notes

(1) Bender, M. L. *Mechanisms of Homogeneous Catalysis from Protons to Proteins*; John Wiley & Sons: New York, 1971; Chapters 2, 4, 5.

(2) (a) Melander, L.; Saunders, W. H. J. *Reaction Rates of Isotopic Molecules*; John Wiley and Sons: New York, 1980; p 152. (b) Bell, R. P. *The Tunnel Effect in Chemistry*; Chapman and Hall: New York, 1980.

(3) Hibbert, F. *Adv. Phys. Org. Chem.* **1986**, *22*, 113.

(4) Scherer, G.; Limbach, H.-H. *J. Am. Chem. Soc.* **1989**, *111*, 5946.

(5) Scherer, G.; Limbach, H.-H. *J. Am. Chem. Soc.* **1994**, *116*, 1230.

(6) Schlabach, M.; Limbach, H.-H.; Bunnenberg, E.; Shu, A. Y. L.; Tolf, B.-R.; Djerassi, C. *J. Am. Chem. Soc.* **1993**, *115*, 4554.

(7) Meschede, L.; Limbach, H.-H. *J. Phy. Chem.* **1991**, *95*, 10267.

(8) Gerritzen, D.; Limbach, H.-H. *J. Am. Chem. Soc.* **1984**, *106*, 869.

(9) (a) Bertie, J. E.; Michaelian, K. H.; Eysel, H. H. *J. Chem. Phy.* **1986**, *85*, 4779. (b) Bertie, J. E.; Michaelian, K. H. *J. Chem. Phy.* **1982**, *76*, 886.

(10) Millikan, R. C.; Pitzer, K. S. *J. Am. Chem. Soc.* **1958**, *80*, 3515.

(11) Kim, Y. *J. Am. Chem. Soc.* **1996**, *118*, 1522.

(12) Grant, R. J. In *The Chemistry of Amidines and Imidates*; Patai, S., Ed.; Wiley: New York, 1975; Chapter 6.

(13) Yamashita, K.; Kaminoyama, M.; Yamabe, T.; Fukui, K. *Theor. Chim. Acta* **1981**, *60*, 303.

(14) Hrouda, V.; Florián, J.; Polášek, M.; Hobza, P. *J. Phys. Chem.* **1994**, *98*, 4742.

(15) Hrouda, V.; Florián, J.; Hobza, P. *J. Phys. Chem.* **1993**, *97*, 1542.

(16) (a) Nguyen, K. A.; Gordon, M. S.; Truhlar, D. G. *J. Am. Chem. Soc.* **1991**, *113*, 1596. (b) Svensson, P.; Bergman, N.-Å.; Ahlberg, P. *J. Chem. Soc., Chem. Commun.* **1990**, 82.

(17) (a) Almenningen, A.; Bastiansen, O.; Motzfeldt, T. *Acta Chem. Scand.* **1970**, *24*, 747. (b) Almenningen, A.; Bastiansen, O.; Motzfeldt, T. *Acta Chem. Scand.* **1969**, *23*, 2848. (c) Harmony, M. D.; Laurie, V. W.; Kuczkowski, R. L.; Schwendeman, R. H.; Ramsay, D. A.; Lovas, F. J.; Lafferty, W. J.; Maki, A. G. *J. Phys. Chem. Ref. Data* **1979**, *8*, 619.

(18) Szczesniak, M.; Scheiner, S. *J. Chem. Phys.* **1992**, *97*, 4586. (b) Luth, K.; Scheiner, S. *J. Chem. Phys.* **1992**, *97*, 7519 (c) Latajka, Z.; Scheiner, *J. Mol. Struct. (THEOCHEM)* **1991**, *234*, 373.

(19) (a) Mijoule, C.; Latajka, Z.; Borgis, D. *Chem. Phys. Lett.* **1993**, *208*, 364. (b) Barone, V.; Orlandini, L.; Adamo, C. *Chem. Phys. Lett.* **1994**, *231*, 295. (c) Smith, B. J.; Radom, L. *Chem. Phys. Lett.* **1994**, *231*, 345.

(20) Ruiz-López, M. F.; Bohr, F.; Martins-Costa, M. T. C.; Rinaldi, D. *Chem. Phys. Lett.* **1994**, *221*, 109.

(21) Frisch, M. J.; Trucks, G. W.; Schlegel, H. B.; Gill, P. M. W.; Johnson, B. G.; Robb, M. A.; Cheeseman, J. R.; Keith, T. A.; Petersson, G. A.; Montgomery, J. A.; Raghavachari, K.; Al-Laham, M. A.; Zakrzewski, V. G.; Ortiz, J. V.; Foresman, J. B.; Cioslowski, J.; Stefanov, B. B.; Nanayakkara, A.; Challacombe, M.; Peng, C. Y.; Ayala, P. Y.; Chen, W.; Wong, M. W.; Andres, J. L.; Replogle, E. S.; Gomperts, R.; Martin, R. L.; Fox, D. J.; Binkley, J. S.; Defrees, D. J.; Baker, J.; Stewart, J. P.; Head-Gordon, M.; Gonzalez, C.; Pople, J. A. GAUSSIAN 94; Gaussian, Inc., Pittsburgh, 1995.

(22) Becke, A. D. *J. Chem. Phys.* **1993**, *98*, 5648.

(23) Lee, C.; Yang, W.; Parr, R. G. *Phys. Rev. B* **1988**, 786.

(24) Onsager, L. *J. Am. Chem. Soc.* **1936**, *58*, 1486.

(25) Tapia, O. In *Molecular Interaction*; Ratajczak, H., Orville-Thomas, W. J., Eds.; Wiley: New York, 1982; Vol. 3, p 47.

(26) Wong, M. W.; Frisch, M. J.; Wiberg, K. B. *J. Am. Chem. Soc.* **1991**, *113*, 4776.

(27) Szafran, M.; Karelson, M. M.; Katritzky, A. R.; Koput, J.; Zerner, M. C. *J. Comput. Chem.* **1993**, *14*, 371.

(28) Rivail, J. L.; Terryn, B.; Rinaldi, D.; Ruiz-Lopez, M. F. *J. Mol. Struct.* **1985**, *120*, 387.

(29) Scheiner, S. In *Reviews in Computational Chemistry*; Lipkowitz, Boyd, D. B., Eds.; VCH: New York, 1991; Vol. 2, p 165.

(30) Boys, S. F.; Bernardi, F. *Mol. Phys.* **1970**, *19*, 55.

(31) (a) Chang, Y.-T.; Yamaguchi, Y.; Miller, W. H.; Schefer, H. F., III. *J. Am. Chem. Soc.* **1987**, *109*, 7245. (b) Shida, N.; Barbara, P. F.; Almlöf, J. *J. Chem. Phys.* **1991**, *94*, 3633. (c) Svensson, P.; Bergman, N.-Å.; Ahlberg, P. *J. Chem. Soc., Chem. Commun.* **1990**, *1990*, 862.

(32) Weast, R. C. *CRC Handbook of Chemistry and Physics*; CRC Press: West Palm Beach, 1979.